In: AIAA SciTech Forum 2023, 23-27 January 2023, National Harbor, Maryland, USA
DOI:10.2514/6.2023-1530

Scheduled Flight Control System of Tilt-Rotor VTOL PAV

Namuk Kang,* James F. Whidborne, † Linghai Lu, ‡ Julien Enconniere§
Cranfield University, Cranfield, Bedfordshire, MK43 0AL, United Kingdom

This paper develops the longitudinal flight control scheme for the tilt-rotor VTOL Aston Martin Volante Vision. It is envisaged that the aircraft will be flown by a "flight-naive pilot" who is less well-trained than normal. The conversion corridor is developed and the optimum tilt schedule is determined using the minimum power curve and numerical optimisation to encompass hover, conversion and cruise flight without manipulating the rotor tilt angle. The methodology is found to be unique because two conversion schedules were integrated to reflect critical factors for conversion and stationary configurations. A proportional-integral-derivative (PID) controller has been designed with a suitable inceptor response and control allocation for a flight-naïve pilot while a blending schedule has unified different response types at the low and high speed into a single control system. The PID controllers are evaluated using design guidelines of ADS-33E-PRF and MIL-STD-1797A. The conversion flight simulation shows that the suggested longitudinal stability and control augmentation system (SCAS) are expected to reduce the pilot workload and improve handling qualities making performance and handling more suitable for a flight-naive pilot.

I. Nomenclature

a_x	=	translational acceleration, m/s^2
A	=	state matrix
B	=	input matrix
g	=	gravitational constant, m/s^2
J	=	cost function
K	=	gain matrix
n	=	rotor rotational speed, rpm
P	=	power, kW
q	=	pitch rate, deg/s
q_{pk}	=	peak pitch rate, deg/s
q_{ss}	=	steady state pitch rate, deg/s
$\overline{q}$	=	dynamic pressure, Pa
T_{θ_2}	=	Incidence lag time constant, s
u	=	body x-axis velocity, m/s
U	=	control input vector
V_{CAS}	=	calibrated airspeed, m/s
V_{stall}	=	stall airspeed, m/s
w	=	body z-axis velocity, m/s
X	=	state variable vector
$\dot{X}$	=	state derivative vector
α	=	angle of attack, deg
γ	=	flight path angle, deg
γ_{tilt}	=	rotor tilt angle, deg
ζ_{sp}	=	short period damping ratio
η	=	elevator deflection, deg
θ	=	pitch attitude, deg
θ_{DB}	=	pitch attitude dropback, deg
θ_{pk}	=	peak pitch attitude, deg
λ_{sp}	=	short period eigenvalue
λ_θ	=	pitch attitude eigenvalue
λ_η	=	elevator eigenvalue
λ_τ	=	rotor lag dynamics eigenvalue
τ_p	=	phase delay, s
ω_{BW}	=	bandwidth frequency, rad/s
ω_n	=	natural frequency, rad/s
ω_{sp}	=	short period frequency, rad/s

*Research Student, Centre for Aeronautics, School of Aerospace, Transport & Manufacturing, namuk.kang@cranfield.ac.uk
†Professor, Centre for Aeronautics, School of Aerospace, Transport & Manufacturing, j.f.whidborne@cranfield.ac.uk
‡Senior Lecturer, Centre for Aeronautics, School of Aerospace, Transport & Manufacturing, l.lu@cranfield.ac.uk
§Research Fellow, Centre for Aeronautics, School of Aerospace, Transport & Manufacturing

II. Introduction

Interest in electric vertical take-off and landing (eVTOL) air vehicles has been increasing as the configuration emerges as a promising candidate for an on-demand service platform through advanced air mobility. Manufacturing companies such as Vertical Aerospace, Lilium and Airbus have already completed successful test flights and Hyundai showcased their first eVTOL vehicles in 2020. In response to the global trends of the aerospace field, Aston Martin presented the Volante Vision Concept as a candidate for the future personal air mobility market. This new concept tiltrotor aircraft seen in Fig. 1 was conceived in partnership with Cranfield Aerospace Solutions, Cranfield University and Rolls-Royce and intended to combine the vertical lift capability of a helicopter with the performance of a conventional fixed-wing aircraft through conversion flight.

Fig. 1 The Aston Martin Volante Vision Concept

The conversion flight control of tiltrotor aircraft is a challenging technical problem because varying flight conditions due to the convertible rotors cause extremely coupled and nonlinear dynamics along with increased modelling uncertainty [1, 2]. Recent research has explored the conversion control strategies of tiltrotor aircraft based on the conversion corridor idea that defines a stable and safe operating range during transition between helicopter configuration and airplane configuration [3–5]. Trim-point analysis can be used to determine the conversion corridor [6, 7]. A satisfactory tilt conversion strategy should ensure a constant altitude whereby decreasing rotor lift is compensated by increasing aerodynamic lift. The tilt rate is also critical because a too low rate can jeopardise the aircraft due to a chance of straying outside the conversion corridor and reaching the line of the power limit, whereas rotating the tilt angle of rotors too fast can result in insufficient lift due to wing stall [8].

Various approaches to controlling and scheduling the tilt angle of convertible aircraft have been proposed [9]. The tilt angle can be linearly scheduled on the airspeed [10–12]. Alternatively, one approach [13, 14] is to schedule the tilt angle to keep the aircraft in the middle of the conversion corridor. Other schemes choose the schedule to minimise thrust-to-weight ratio [15] or to reduce excursion to pitch attitude [16]. A manual approach using a thumbwheel and a discrete beep trimmer has been proposed for piloted aircraft [17]. For the XV-15, the pilot can operate the conversion procedure at a constant and continuous tilt rate but manual access is available in the case of an emergency halt at any nacelle tilt angle or convert to the helicopter mode [3]. Both the AW609 and Bell-Boeing V-22 Osprey have adopted a conversion protection system (CPS) to prevent crossing the boundaries of the conversion corridor. The tilting control regime of AW609 depends on the nacelle tilt angle [4]. For the V-22, the boundaries of the tilt corridor vary with the gross weight so that the CPS covers flexible operation over the full envelope [5].

Classical control techniques have been proposed for the flight control of tiltrotor aircraft over the whole flight envelope; PID control is a common approach. With the aid of PID controller, quad tilt-wing unmanned air vehicle employed independent control unit of wings and rotors [18, 19] while a similar tilt-wing vehicle can tilt propellers and wings simultaneously [20]. An air vehicle with three tilting rotors was developed in the study [21, 22] and it was observed that the helicopter mode of the tiltrotor vehicles mostly used attitude and position control [18–22].

Table 1 Recommended stick input type for a PAV depending on dynamic pressure [26]

Stick input type	$\overline{q}$	Command type
Left longitudinal stick	Low	Horizontal ground velocity
	Medium	Throttle and pitch
	High	Pure throttle
Right longitudinal stick	Low	Vertical ground velocity
	Medium	As per low dynamic pressure
	High	As per low dynamic pressure

Human factors are also critical for the operation of piloted VTOL aircraft given that it becomes more difficult to pilot two different configurations in a single vehicle [12]. The requirements are even more significant because, in order for the future personal air mobility market to be commercially viable, so-called "flight-naïve pilots" will be mostly employed and they are pilots with more limited training that requires skill levels similar to those required to drive an automobile [23]. The study by Perfect et al., [24] revealed the most suitable response types for personal air vehicle (PAV) configurations piloted by novices were translational rate command (TRC) and acceleration command speed hold (ACSH) according to the assessment of NASA task load index (TLX) [25] and task performance index (TPX) [26]. Analogously to the proposed response types, the novel inceptor design for PAV based on the Cooper-Harper rating (CHR) was as suggested in Table 1.

As yet there are no published standards that cover numerical requirements and handling qualities design guidance for tiltrotor aircraft. Therefore, the compatibility analysis is to balance the criteria of both fixed-wing aircraft and rotorcraft so that conversion flight remains robust and qualitative [27]. MIL-STD-1797A [28] is the applicable specification for flying and handling qualities of fixed-wing aircraft. For military rotorcraft, the criteria are stipulated in ADS-33E-PRF [29]. For the pitch-axis response criteria in the time domain, the requirements for the mid-term response specify the region of stability in terms of damping ratio and natural frequency. Also, the specification regulates the minimum control power and quickness for rate response rapidity type by inspection of parameters related to time-domain pitch response.

Frequency-domain criteria are also significant because reasonable time-domain responses may produce unacceptable flying qualities if frequency-domain properties are ignored. Therefore, bandwidth criteria suggest the required bandwidth frequency and phase delay to rectify potential issues that cannot be dealt with in the time domain. However, the assessment of handling qualities in the specifications is intended for experienced pilots. Considering the aircraft is for urban air operations, additional focus on those with private pilot's license and insufficient flight experience should be made in the flight control system when referring to the specifications.

This paper considers the scheduled flight control system of the Aston Martin Volante Vision concept VTOL vehicle for flight-naive pilots. Firstly, inherent dynamics characteristics based on straight and wing-level trim states are examined and conversion corridor analysis is employed to determine the optimum tilt schedule. One approach for safety is to keep the tilt schedule in the centre of conversion boundaries at a small angle of attack, which is important for conversion flight. However, this method is more costly in terms of power consumption and not suitable for hover and cruise configurations. Hence, a compromise between the two approaches is proposed in this paper. Flight simulation is used to assess whether a gain-scheduled PID controller can maintain stable conversion along the tilt schedule without altitude loss. The approach of using an optimum tilt schedule in this paper means that the flight configuration is automatically switched based on the calibrated airspeed. This is expected to enhance handling qualities and reduce pilot workload, making the system easier for the pilot along with a possible decrease in pilot training hours compared to conventional piloting techniques [26, 30].

III. Flight dynamics analysis

A. Dynamic model and trim analysis

The configuration of the Aston Martin Volante Vision is shown in Fig. 2. The main rotor is located aft of the cockpit and has a fixed tilt but is electrically driven with a variable speed. The blade pitch is also fixed. The forward tilt rotor pairs are counter-rotating and can be tilted about the Y-axis. They are also electrically driven with a fixed blade pitch

but variable speed. The aircraft is fitted with canards, but trailing edge elevators on the main wing are provided. The main wing also has outboard ailerons and rudders on the fin.

In the low-speed hover configuration, the main rotor and the tilt rotor pair provide the lift. Differential and collective use of the main and tilt rotor speeds provide pitch and heave control. Conversion from the hover configuration to the fixed-wing aircraft configuration is enabled by varying the tilt angles so rotating the fore rotor thrust vector direction. This provides some surge control. The lifting surfaces have a sufficient aerodynamic lift to support the weight at high speed in the fixed-wing aircraft configuration and the main rotor becomes redundant. The tilt rotors provide forward thrust to accelerate the aircraft. The main wing trailing edge elevator is employed instead of the canard to control pitch in the fixed-wing aircraft configuration.

A model was previously developed in the study [31]; the main aircraft model parameters are summarised in Table 2. The aerodynamic forces and moments characteristics were modelled using Athena Vortex Lattice (AVL) [32] to obtain the aeroderivatives while a blade element momentum theory solver called QPROP [33] was employed to predict the performance of the rotor thrust along with semi-empirical correction [34]. Note that the model ignores viscous effects, nonlinearity, and accuracy of excessive blade angle of attack, which limits its fidelity in the full flight envelope.

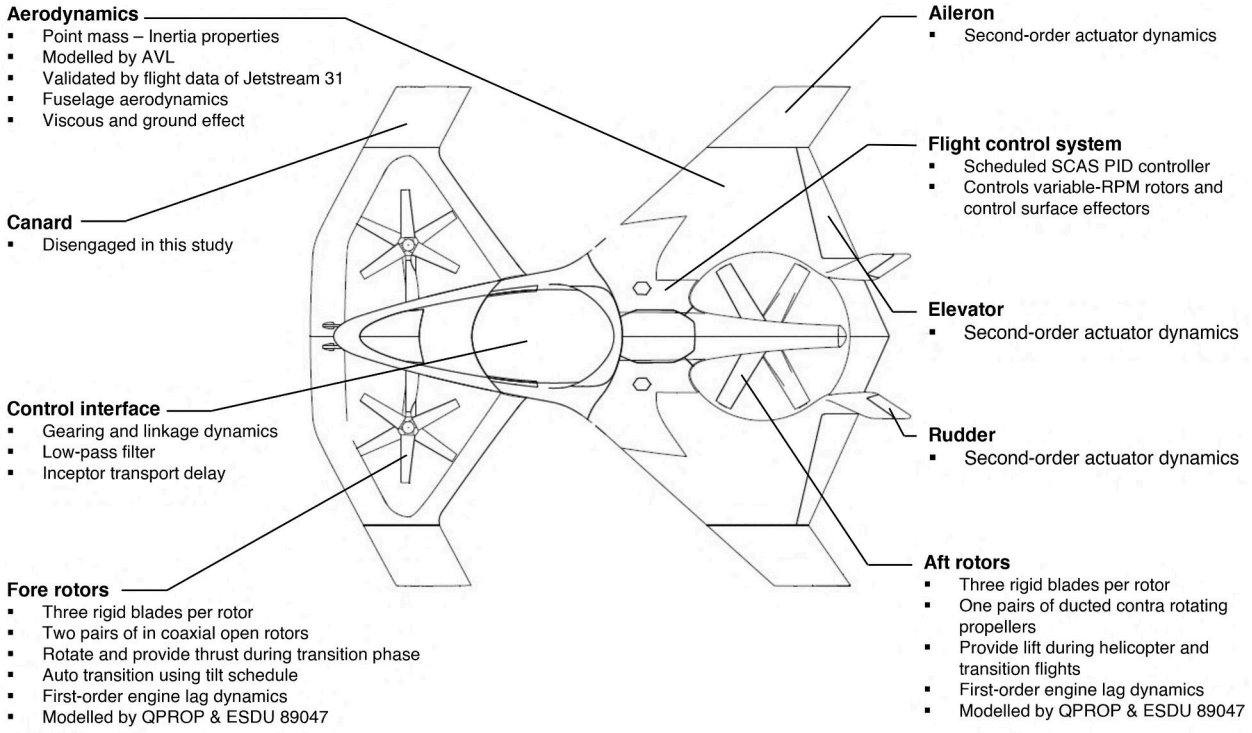

Fig. 2 Schematic of the Volante Vision

Trim analysis for steady wings-level flight is a prerequisite to the design of the conversion corridor. Numerical trimming using a nonlinear least-squares solver was performed over the entire range of operational airspeed and rotor tilt angle. The trim was set so that the power is minimised at each trim point. The main rotor speed was set to be zero above the stall speed of 41 m $s^{-1}$to maximise the aerodynamic forces and minimise the use of a powered lift for saving energy. The maximum limits on pitch and angle of attack were arbitrarily chosen to be 20 deg as a constraint on passenger comfort and safety. The resulting trim contours at an altitude of 1000 m are shown in Fig. 3 and 4. Lateral and directional flight dynamics states and control inputs were found to be decoupled from the longitudinal.

The control inputs and power trim values are shown in Fig. 3. Even though the main rotor rotational speed was suppressed to zero against increasing freedoms of the elevator above the stall speed, the other trim result contours still varied smoothly despite the different trim condition. The phenomenon implied that the trim conditions were still valid to be combined between the two trimming results and the powered-lift forces should be avoided as much as possible above the stall speed to minimise power consumption.

Table 2 Model parameters of Aston Martin Volante Vision

Symbol	Description	Magnitude
m_{MTOW}	maximum takeoff weight	2000 kg
I_{xx}	moment of inertia at x axis	10608 kg m^2
I_{yy}	moment of inertia at y axis	35554 kg m^2
I_{zz}	moment of inertia at z axis	45921 kg m^2
I_{xz}	moment of inertia on xz plane	447 kg m^2
CG	centre of gravity from nose	4.45 m
V_{max}	maximum true airspeed	97 m s^{-1}

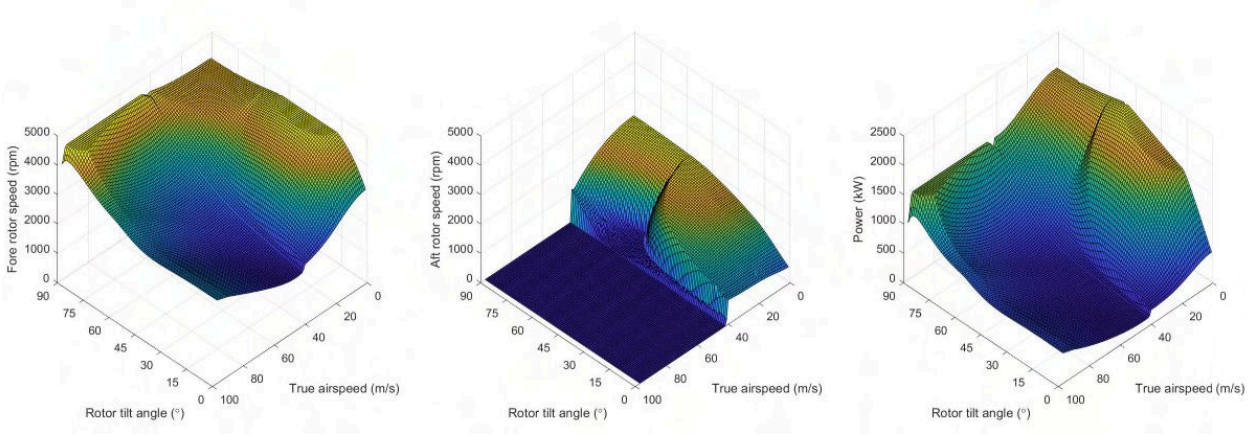

Fig. 3 Trimming result contours of power and rotor rpm

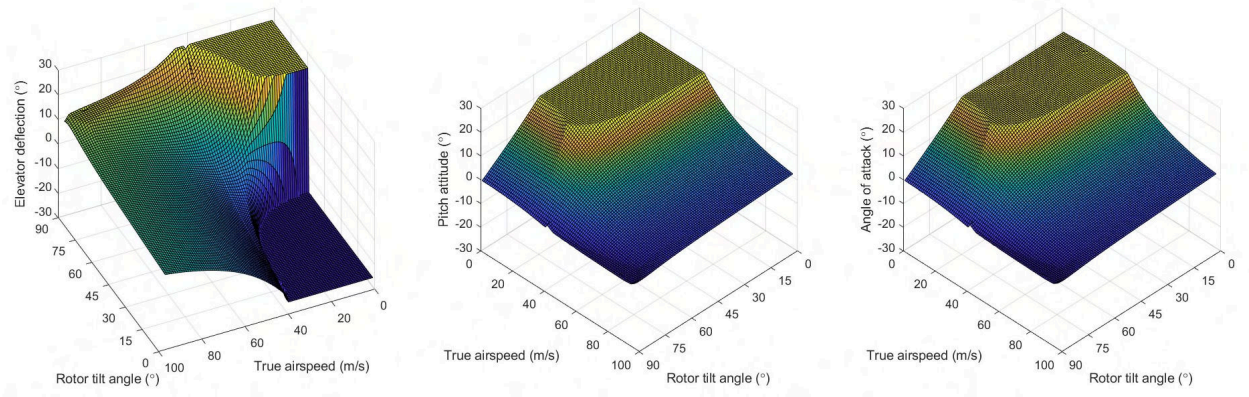

Fig. 4 Trimming result contours of elevator deflection, pitch attitude and angle of attack

With reference to Fig. 4 and 5, the elevator deflects downward to its maximum to exert the possible maximum aerodynamic force from lifting surfaces and battery efficiency in the helicopter configuration at low cruise speed. Additionally, the maximum negative deflection of the upward elevator occurred at low speed to generate the maximum pitching moment from the control surfaces and to counter the opposite moment due to the main rotor thrust, which leads to an untrimmed region caused by a low rotor tilt angle. Also, the fore rotor speed reached its maximum at another untrimmed region at high speed and rotor tilt angle. Consequently, there were two untrimmed flight regions; one from the stall speed region, the other due to the limit on the maximum power of the rotors to counter the aerodynamic forces from the wing.

It is noticeable that the lower the rotor tilt angle of the front rotor was positioned, the higher the required angle of attack was at the same airspeed. Furthermore, the angle of attack kept increasing until it reached the maximum limit of the trim condition, which contributed to the untrimmed region below the stall speed. The aircraft may be able to fly above the upper limit using rotor thrust, but such flight is undesirable because a high pitch attitude of the aircraft in the region loses the efficiency of the powered lifts at the low speed and would not guarantee a stable flight against a gust.

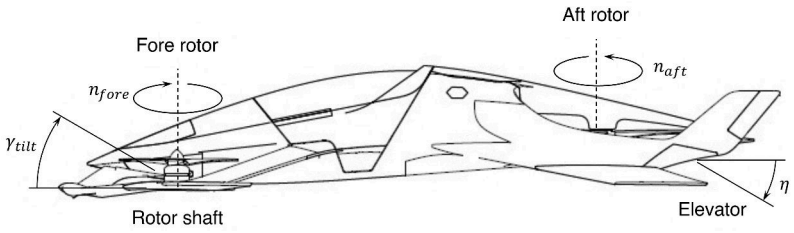

Fig. 5 Longitudinal control configuration of the Volante Vision

B. Conversion corridor design

The operational conversion (or transition) flight region of the aircraft was designed based on the calibrated airspeed in order that the mapping of the conversion envelope to be established could suggest valid data irrespective of the altitude. The extent to which each point in the trim results can assure the aircraft of its stability was determined by selecting the local trim results for the conversion corridor under the best passenger comfort ratings according to the study in terms of acceleration [35]. The resulting conversion corridor is presented in Fig. 6 with two tilt corridor boundaries. The upper boundary was constrained by the limit of the power, whereas the minimum speed to be avoided was determined by the lower boundary. Although the transition flight is not supposed to be in the trimmed flight but accelerating or decelerating, the operational conversion region inside the boundaries is still expected to provide the relative stability of the conversion flight.

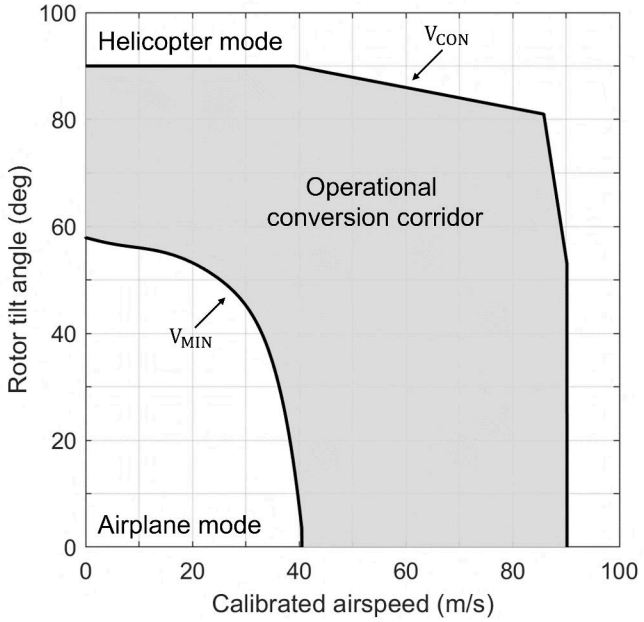

Fig. 6 The conversion corridor for the Volante Vision

C. Tilt schedule

According to [13], the tilt schedule not only facilitates automatic transition but also prevents the aircraft from excessively exceeding the conversion corridor. For the design of the tilt schedule, the minimum power curve within the conversion corridor boundaries was obtained by the inspection of local trim points that feature the minimum power at each calibrated speed from 0 to 90 m s^{-1} with an interval of 1 m s^{-1}. The resulting plot is shown in Fig. 7. Concerning the minimum power line, it shows that tilting the front rotors forward immediately is the optimum strategy to maximise the power efficiency after remaining at the hover configuration up to 3.81 m s^{-1}. When exceeding the stall speed, the minimum power indicates that the rotor tilt angle needs to be increased again, not holding with the fixed-wing aircraft configuration. This is because a more upward elevator deflection is required to counter the negative pitching moment due to the excessive amount of the aft wing-aerodynamic lift force. This also explains the reason why the fore rotors are not positioned horizontally to balance the negative pitching moment analogously to the elevator. Consequently, the complete cruise flight configuration uses less elevator to provide the lift forces.

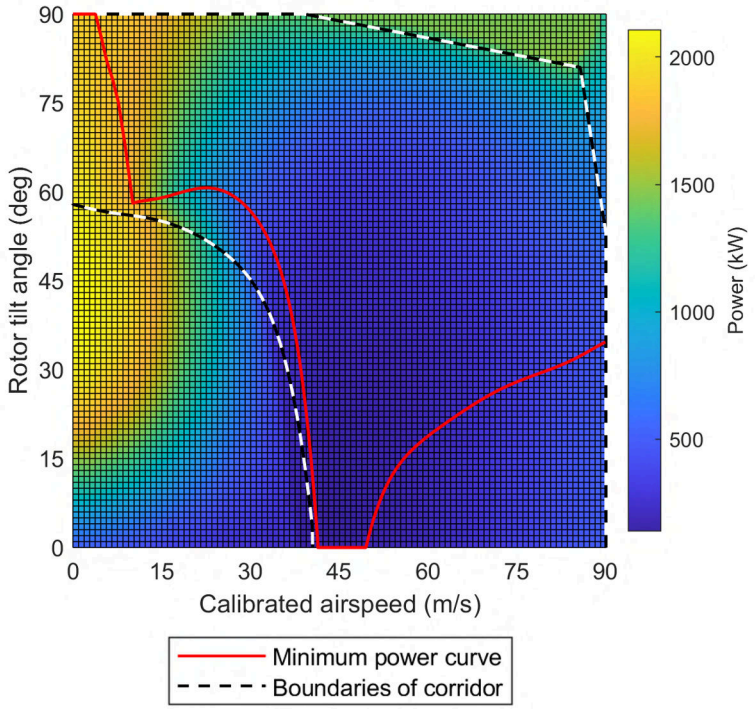

Fig. 7 Minimum power curve with conversion corridor

Using only the minimum power curve as the tilt schedule benefits the power consumption. However, the curve is close to the minimum speed boundary and the stall region, which could jeopardise the aircraft. Hence, a term is added to the cost that penalises the deviation angle of attack from 4 deg to trade off between the minimum power and safety. The fixed angle of attack was chosen in the weighted sum because it is a typical value for a cruise flight and presented the centre of the two boundaries and a margin for operational limit. However, the choice of the optimum angle of attack is for future study. The optimisation goal was to establish a tilt schedule that enables smooth conversion and reaches the cruise flight configuration with a constant angle of attack. The optimum points were obtained by numerical search to minimise the following weighted sum:

$$J(\alpha, P) = \frac{|\alpha(\gamma_{tilt}, V_{CAS}) - 4|}{\max(\alpha(\gamma_{tilt}, V_{CAS}))} + \frac{P(\gamma_{tilt}, V_{CAS})}{\max(P(\gamma_{tilt}, V_{CAS})} \tag{1}$$

s.t.

$$\forall \gamma_{tilt} = \{1, 2, ..., 90\} \text{ for } V_{CAS} = 1, 2, ..., 90$$

The optimisation procedure is designed to minimise the nondimensional sum of the angle of attack and the minimum required power. The absolute value of angle of attack was set up to avoid negative magnitude and each calibrated airspeed ranging from 0 m s^{-1} to 90 m s^{-1} identified the rotor tilt angle that possesses the least value of the cost function within the conversion corridor boundaries. The result of the optimisation is presented in Fig. 8 and indicates that the obtained transition flight curve leads to the minimum power consumption with an angle of attack close to 4 deg.

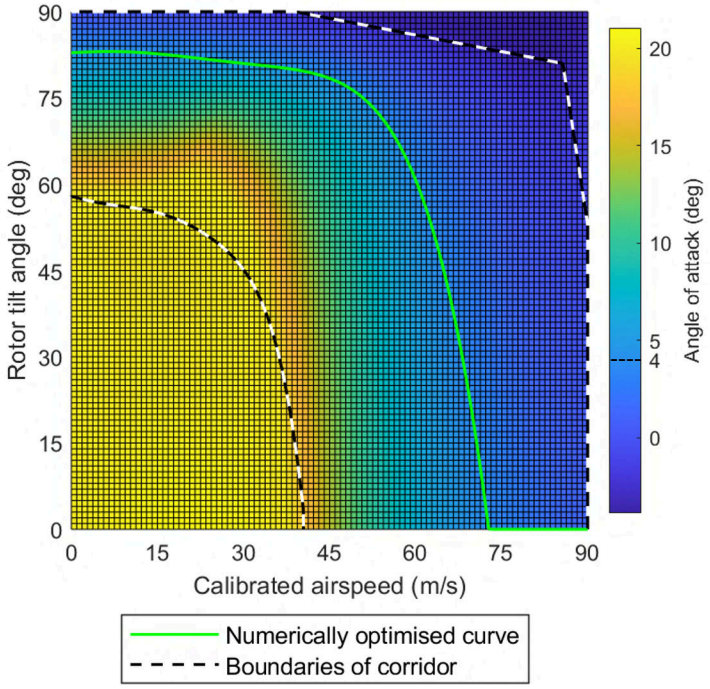

Fig. 8 Numerically optimised curve with conversion corridor

At hover, the aircraft operates as a rotary-wing craft, hence with zero angle of attack. Thus, there is a disconnect between the numerically optimised curve and the requirement for rotary-wing operation. Therefore, the minimum power and numerically optimised curve were integrated to modulate all configurations with a single tilt schedule. The tilting strategy is expected to enhance handling qualities by reducing pilot workloads without manipulation of a flight state switch [26] and not to structurally burden the actuators for conversion with no use of the rotor tilt angle as a primary control variable in the cockpit [17] in real piloted flight. An exponential function (shown in Table 3) is defined to provide a smooth transition from the rotary-wing schedule to the numerically optimised curve schedule. The revised tilt schedule and specific equations are shown in Fig. 9 and Table 3, respectively.

Table 3 Details of the tilt-schedule function

Airspeed range (m s^{-1})	Configuration	$\gamma_{tilt}(V_{CAS})$ (deg)
$0 \leq V_{CAS} < 3.81$	Rotary-wing	90
$3.81 \leq V_{CAS} < 35.3$	Conversion	$e^{-0.05(V_{CAS}-52.39)+78.65}$
$35.3 \leq V_{CAS} < 73.5$	Conversion	$aV_{CAS}^5 + bV_{CAS}^4 + cV_{CAS}^3 + dV_{CAS}^2 + eV_{CAS} + f$
		$a = -1.98 \times 10^{-7}$ $b = 1.78 \times 10^{-5}$ $c = -4.55 \times 10^{-4}$,
		$d = -8.08 \times 10^{-4}$ $e = 0.05$ $f = 83.44$
$73.5 \leq V_{CAS} < 90.2$	Fixed-wing	0

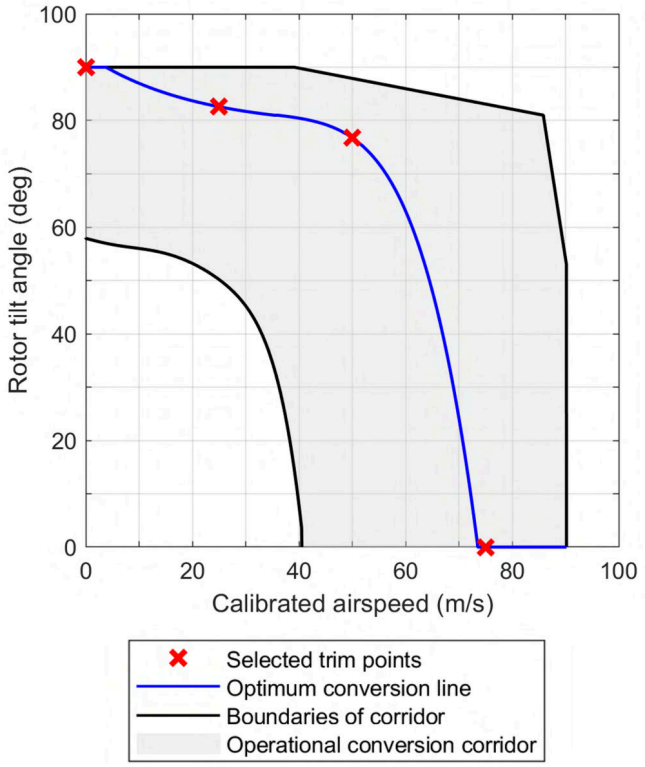

Fig. 9 Optimum tilt schedule for conversion flight with four trim points

IV. Longitudinal SCAS design

A. Linearisation

The proposed control scheme is a gain-scheduled linear PID controller. Linear models were obtained by forming linear approximations to non-linear systems and the linearisation of a system is accessible by the straight and level flight trim points(i.e., equilibrium points). Four trim point flight conditions on the tilt schedule were selected at the calibrated airspeeds of 0, 25, 50, and 75 m s^{-1} to assess the system stability and design the flight control system. The detailed flight conditions to be analysed are shown in Fig. 9 and Table 4.

Table 4 Flight condition data of the trim points

	Flight Case			
	1	2	3	4
Altitude (m)	1000	1000	1000	1000
Calibrated airspeed (m s^{-1})	0	25	50	75
Pitch attitude (deg)	0	3.7	3.59	3.5
Rotor tilt angle (deg)	90	82.6	76.8	0
Fore rotor speed (rpm)	4155	4146	3500	2410
Aft rotor speed (rpm)	2196	1466	0	0
Elevator (deg)	0	25	6.36	-2.4
Power (kW)	1916	1365	686	325

The aerodynamic coupling derivatives were close to zero, hence the lateral and longitudinal equations of motion are decoupled and only the longitudinal dynamics are considered for this conversion strategy. The aircraft was numerically linearised about four steady-state operating points so that the gradient (i.e., Jacobian) matrices were calculated from the Simulink model.

B. Motor mixing algorithm and controllability

In the proposed control system for the Volante Vision at low airspeed, two different types of control are applied to provide body-axis horizontal and normal velocity command; the attitude controller and the velocity controller. Therefore, a motor mixing algorithm was introduced for the outputs to follow the reference signal by demanding multiple rotor speeds simultaneously. For vertical rate command (VRC), a combined engagement of both rotors as a collective input controls the vertical velocity command by offsetting a pitching moment due to each rotor thrust. However, a high-bandwidth surge control force for pure TRC is absent in the longitudinal characteristics; the tilt mechanism is reserved for the conversion. Thus, pitching down the aircraft alternatively provides a body-axis horizontal velocity command using the differential control input of the tilt and main rotors.

Referring to ADS-33E-PRF, the gains of the tilt and main rotors were selected to generate a pitch rate of 1 deg s^{-1} and a normal acceleration of 0.05 g without the coupling effects between them. The gain scheduling was designed only for Flight Cases 1 and 2 before the aircraft reaches $1.2V_{stall}$ because the rear rotor thrust with a positive angle of attack exhibits a considerable negative translational acceleration and the forward flight control scheme will take over the control authority. The resulting gain scheduling of the mixed input using the tilt and rear rotor is shown in Fig. 10. Controllability was checked and found that the system was state controllable and all the modes of the system were found to be under the influence of the control inputs.

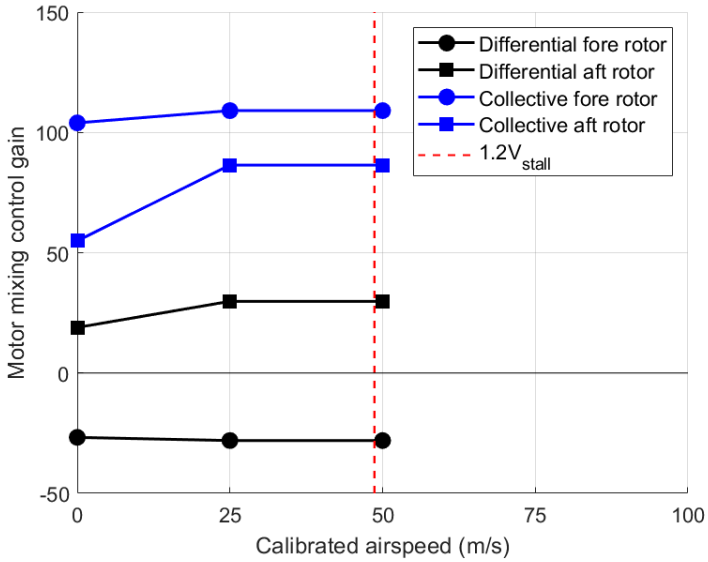

Fig. 10 Gain scheduling for differential and collective input

C. Stability augmentation system

The short-term response behaviours are more important than the phugoid mode in terms of flying and handling qualities. Reduced-order models for the short period mode were therefore developed in the body-axes reference. Flight Case 1 represents hovering dynamics and the contribution of the vertical motion to the longitudinal mode is less than 10 percent of the horizontal speed [8]. Hence, a reduced-order model can be obtained by ignoring the normal velocity. For the other flight cases, the short period mode is mainly dominated by pitch rate q and incidence α. The x-axis force equation can be therefore neglected due to the constant speed u in the rapid pitch oscillation. The reduced order model of the Volante Vision was obtained with the linear model form:

$$
\begin{aligned}
&\dot{X} = AX + BU \\
&\text{where} \\
&X = [u\ q\ \theta]^T \text{ for Flight Case 1} \\
&X = [w\ q\ \theta]^T \text{ for Flight Cases 2, 3 and 4} \\
&U = [\gamma_{tilt}\ n_{fore}\ n_{aft}\ \eta]^T
\end{aligned} \tag{2}
$$

The resulting short-term stability and response characteristics are presented in Table 5. An engine lag and actuator dynamics were augmented to the model. Overall, the bare-airframe short period mode damping ratio is low and fairly constant with increasing airspeed, but the natural frequency increases from 0.105 to 2.93 rad s^{-1}. Flight Cases 1 and 2 have too low short period frequencies and the bare airframe dynamics of all four flight cases possess poor performance that will be described in the next paragraph. Stability augmentation is necessary when the aircraft shows intrusive deficiencies of the bare airframe dynamics and choosing proper feedback can provide the aircraft with the enhanced closed-loop stability modes [36]. Hence, the pitch rate feedback gain was determined using the root-locus technique to improve the dynamics and closed-loop system analysis was accessible through:

$$\dot{X} = (A - BK)X + BU \tag{3}$$

For Flight Cases 1 and 2, pitch attitude is fed back along with pitch rate because pitch rate feedback alone could not achieve the short-period mode stability requirement. Also, a step cockpit pitch control position input is recommended for TRC and flight path response according to ADS-33E-PRF [29]. Feedback gains of the pitch attitude and rate were chosen to attain the highest level of handing qualities based on the limit on pitch oscillation 16 17, requirements for moderate-amplitude pitch attitude changes 18, and bandwidth criterion 20 21 referring to ADS-33E-PRF [29] and MIL-STD-1797A [28], simultaneously. The results of the evaluation are discussed in the further section.

Table 5 Bare airframe and closed-loop characteristics of the Volante Vision

	Flight Case			
	1	2	3	4
	Bare airframe			
ω_{sp}	0.105	1.01	1.97	2.93
ζ_{sp}	0.512	0.472	0.473	0.480
λ_τ	-10	-10	N/A	N/A
λ_η	N/A	N/A	$-36 \pm 27i$	$-36 \pm 27i$
λ_{sp}	$-0.0536 \pm 0.0897i$	$-0.479 \pm 0.896i$	$-0.932 \pm 1.74i$	$-1.41 \pm 2.57i$
	Closed loop			
ω_{sp}	4.44	4.59	2.19	3.28
ζ_{sp}	0.855	0.758	0.7	0.699
λ_{sp}	$-3.80 \pm 2.30i$	$-3.48 \pm 2.99i$	$-1.53 \pm 1.56i$	$-2.30 \pm 2.34i$

D. Control augmentation system

A conversion flight needs to ensure the integration of two different aircraft configurations and dissimilar primary inceptor response-types in an intuitive way. Referring to the studies [23, 26], a suitable inceptor design for PAV and response type for a flight naïve pilot reached some consensus so that a pilot workload can be alleviated along with the improvement in handling qualities. Table 6 summarises the resulting control scheme of the inceptor response-types and control allocation methodology provided left and right longitudinal sticks are longitudinal cyclic control input and collective lever control input, respectively.

For Flight Case 2, the collective input was adopted to control a flight path angle because the positive sign of γ_{ss}/V_{ss} recommended employing collective control channel rather than pitch channel and a body-axis coordinate is more beneficial in the forward flight according to ADS-33E-PRF. A blending schedule was introduced to connect two

Table 6 Inceptor response-types and control allocation method

Flight Case	Control allocation	Left longitudinal stick	Right longitudinal stick
1	Helicopter mode	TRC (differential thrust)	VRC (collective thrust)
		Blending schedule	
		3.81 m s^{-1} < V_{CAS} < 7.24 m s^{-1}	
2	Helicopter mode	ACSH (differential thrust)	γC (collective thrust)
	Primary control switch		
	$V_{CAS} = 1.2V_{stall}$ = 48.66 m s^{-1}		
3	Wing borne mode	ACSH (fore collective thrust)	γC (elevator)
		Tilt compensator	
		γ_{tilt} > 45 deg and a_x < cyclic input	
4	Wing borne mode	ACSH (fore collective thrust)	γC (elevator)

different types of response in the same aircraft configuration mode. When exceeding $1.2V_{stall}$, the elevator begins to take an authority for the control of flight path angle and a thrust of fore rotor starts to produce an acceleration command speed hold response type. Particularly, a tilting compensator is activated temporarily in the airplane mode before the rotor tilt angle of 45 deg. The compensator employed the mixed inputs of a thrust and tilt angles of the front rotors and assisted the aircraft only in accelerating considering that the thrust is not expected to produce a pure acceleration and follow the longitudinal left stick command due to the rotor tilt angle.

ADS-33E-PRF [29] recommendation on blending schedules suggests that the blending function should be linear with time and occur between 2 and 5 seconds during acceleration. Two specific airspeeds were used to design the blending. One was 3.81 m s^{-1} where the end of rotor tilt angle for the complete helicopter mode was proposed by the tilt schedule. The other was calculated to be 7.24 m s^{-1} by assuming an acceleration of 0.1 g is being maintained for 3 seconds. The resulting blending schedules are shown in Fig. 11.

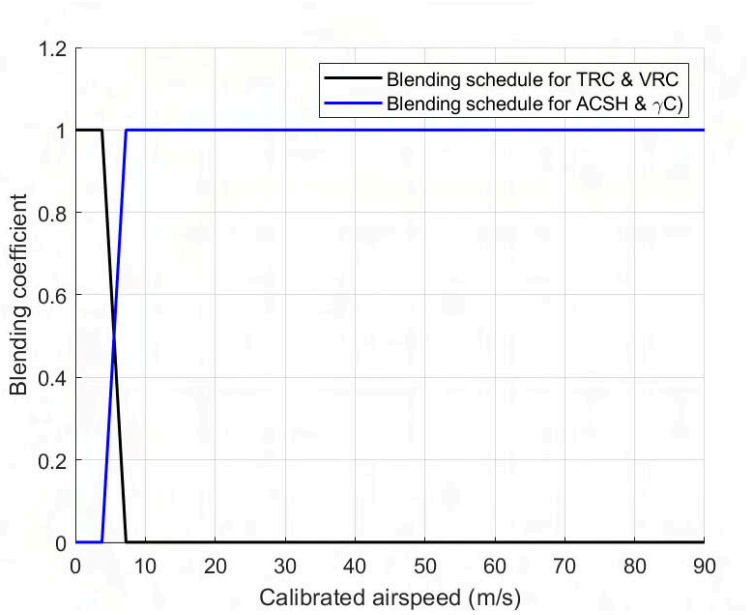

Fig. 11 Blending schedule for different response types

When tuning PID gains, the tilt schedule was frozen to identify the coupling effect between the control channels and assess the performance of the response as a priority. With regards to Flight Case 1, both TRC and VRC were achievable through a coordinate conversion from an earth-fixed framework to a body-fixed axis system. The gains were selected to

satisfy the handling qualities requirements from ADS-33E-PRF [29]. The two response-types were tuned to have a quality first-order shape. The rise time of TRC belonged to the range between 2.5 and 5 seconds as suggested, whereas the height response had a prompter performance than the requirement for the boundary of level 1 handling qualities. As a result, Fig. 12 and 13 showed that both response-types were able to obtain satisfactory responses without an excessive overshoot was achieved along with the qualitative compliance against ADS-33E-PRF.

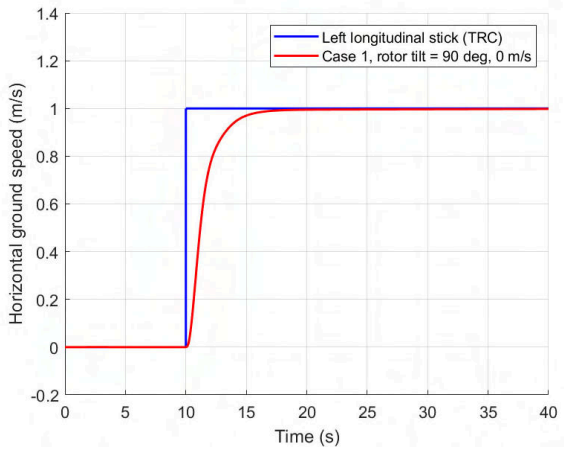

Fig. 12 TRC step response to left stick

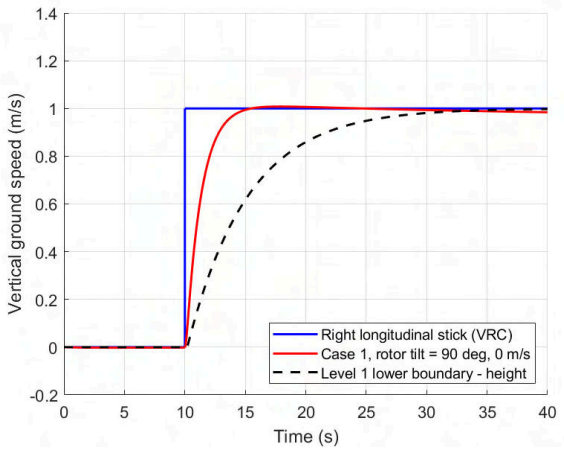

Fig. 13 VRC step response to right stick

The remaining flight cases are designed to provide ACSH and flight path angle response. The gains for the ACSH response are tuned to have a settling time of 10 seconds, which was not thought to be aggressive for the passenger aircraft. A pulse input of 0.05 g was exerted for 15 seconds to prevent intrusive nonlinear effects. The gains for flight path response were determined with reference to ADS-33E-PRF so that the response has a first-order appearance and fulfils the requirements for level 1 handling qualities, analogously to VRC. In Flight Case 4, a command path pre-filter was additionally designed to lower incidence lag and flight path delay by reducing the dropback to near zero 19.

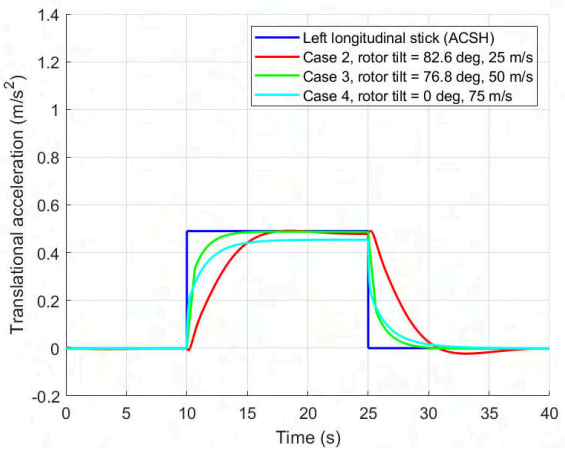

Fig. 14 ACSH pulse response to left stick

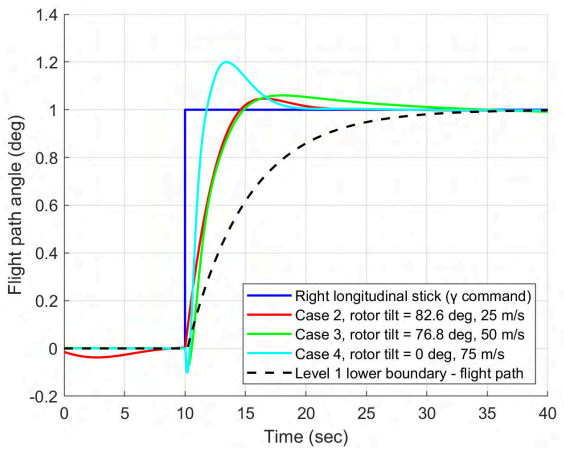

Fig. 15 Flight path step response to right stick

The resulting responses are presented in Fig. 14 and 15. For the pulse response to the left longitudinal stick at Flight Case 4, a steady-state error of around 10 percent was discerned and found to be an unavoidable ACSH response due to insufficient control power to overcome increasing aerodynamic drag. However, this property is acceptable because the pilot or a gearing ratio can compensate for the gap between the reference command and response. By inspection of the step response to the right longitudinal stick, a negative dropback was not spotted as desired and the design considerations were overall well reflected in the response despite a minor overshoot.

V. Handling qualities assessment and flight simulation

A. Handling qualities assessment

Flight-naïve pilots instead of professional pilots will be needed to fly VTOL aircraft for advanced air mobility. This requires more than level 1 to confer reliable stability and control characteristics on its operational flight envelope. The European Aviation Safety Agency (EASA) developed several issues of means of compliance with the special conditions for VTOL aircraft in a sequential manner [37–40]. The Federal Aviation Administration (FAA) is taking modifying approach to tailor the existing regulatory document for the aircraft as special class in 14 code of federal regulations (CFR)§21.17(b) [41]. However, quantitative handling qualities requirements for VTOL aircraft are not yet stipulated in these documents. It should be therefore noted that the helicopter and conversion modes were compared with ADS-33E-PRF, whereas MIL-STD-1797A was referred to the fixed-wing configuration in this paper.

A flight control system with SCAS engaged should acquire level 1 and bare airframe needs to at least meet level 2 handling qualities. As discussed in the preceding sections, the gain selections for the pitch stabilisation were aimed to achieve desirable handling qualities in the time and frequency domains. Figures 16 and 17 summarise the compliance results of pitch dynamic stability requirements, in which the aircraft belonged to category B based on its normal manoeuvre in MIL-STD-1797A. It was confirmed that the flight control system was equipped with the satisfactory handling qualities of level 1 in SCAS design and level 2 at least in bare-airframe system regardless of the aircraft configuration.

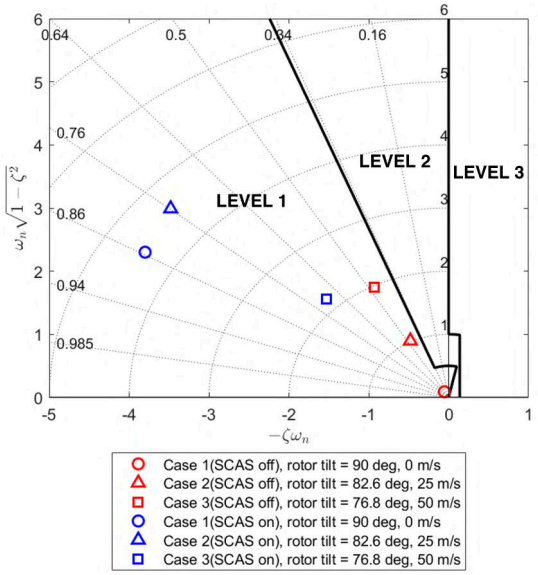

Fig. 16 Compliance results of the short period characteristics (ADS-33E-PRF)

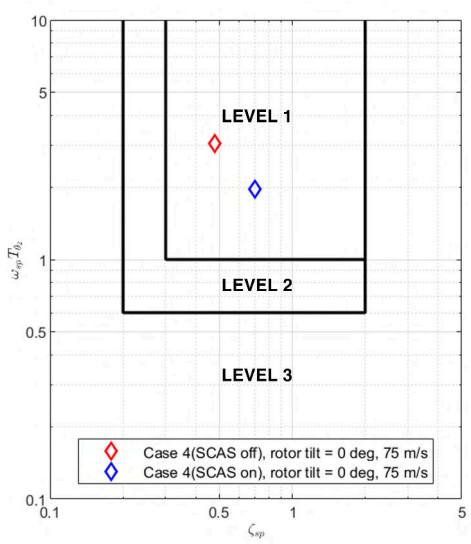

Fig. 17 Compliance results of the short period characteristics (MIL-STD-1797A - flight category B)

With regards to the pitch quickness criterion, it is a unique analysis tool for a rotorcraft because the criterion intends to identify the level of agility near the earth at a low speed. Figure 18 shows handling qualities results of the Volante Vision in the moderate-amplitude pitch attitude quickness requirements in the time domain. Flight Case 4, the fixed-wing configuration, was not included and the remaining three cases lie in level 1 handling qualities. The dropback criterion is applicable for fixed-wing configuration and concerned with the pitch attitude tracking handling quality in terms of the restriction of pitch rate overshoot ratio and the ratio of attitude dropback to steady-state pitch. The closed-loop system for Flight Case 4 augmented a command path pre-filter to achieve zero dropback and relieve flight path response delay. Artificial modification of incidence lag was completed using pole-zero cancellation and the dropback characteristics were quantified by inspection of the moment when the step input to pitch rate is detached. The compliance results are presented in Fig. 19 and Flight Case 4 lies in the satisfactory region away from abrupt bobble tendency.

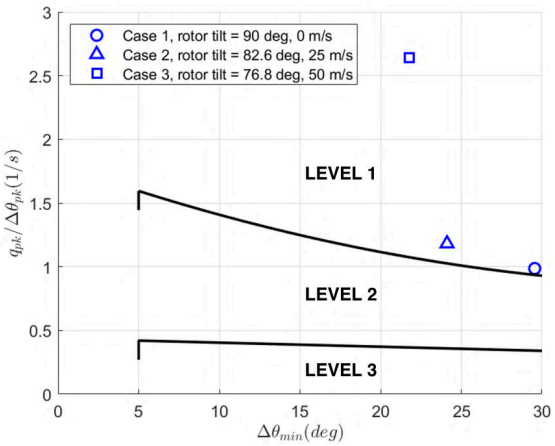

Fig. 18 Handling qualities rating of pitch quickness

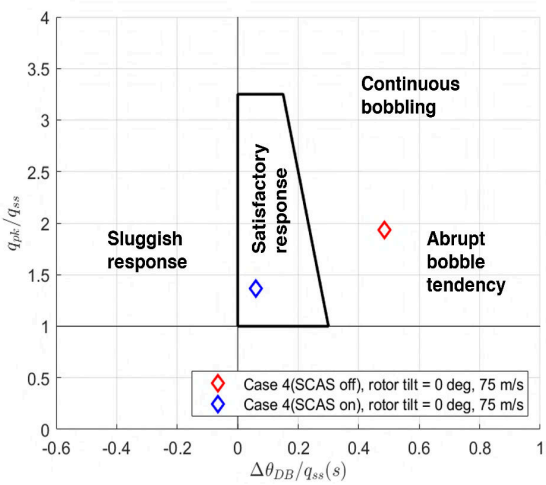

Fig. 19 Handling qualities rating for the Gibson's drop-back criterion

The bandwidth criteria of a rotorcraft vary with mission task elements (MTEs) and the characteristics of the flight control system were compared with the requirement in divided attention operations, considering the aircraft could experience instrument meteorological conditions (IMC). Additionally, Flight Case 4 referred to the requirements for category C because MIL-STD-1797A does not cover flight phase category B and the Volante Vision will not be exposed in the expected operation for category A. The results predict the Volante Vision exhibits level 1 pitch flying qualities shown in Fig. 20 and 21. The bandwidth frequency of Flight Case 4 is the highest even though no pitch attitude feedback is provided. This demonstrates that the fixed aircraft configuration is more controllable than the rotary-wing configuration. Furthermore, the ratings in the bandwidth and quickness criteria show that sufficient bandwidth can correspond to quicker response because it allows the channel to pass large information. Considering a novel concept of aircraft is not covered in compliance with the specifications, a piloted simulation with SCAS on should be conducted to demonstrate that the predicted rating is consistent with the actual performance of MTEs.

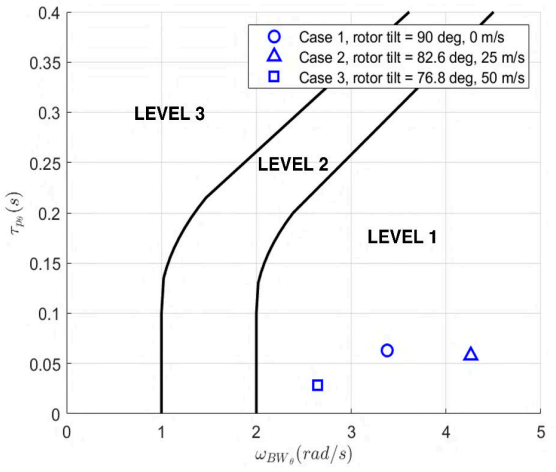

Fig. 20 The pitch attitude bandwidth requirement results (ADS-33E-PRF - all the other MTEs-UCE>1 and/or divided attention operations

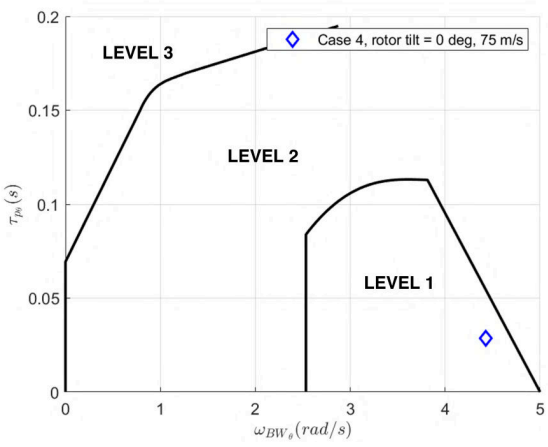

Fig. 21 The pitch attitude bandwidth requirement results (MIL-STD-1797A - flight category C

B. Conversion flight simulation

A 150 seconds flight simulation was performed and the dynamics responses during the full conversion procedure are provided in Fig. 22. The left longitudinal stick input is applied for 135 seconds to accelerate the aircraft at an overall rate of 0.05 g and reaches the fixed-wing aircraft configuration. The right longitudinal stick is exerted to maintain the altitude of 1000 m during the conversion at around 100 seconds. When the aircraft reached the cruise flight configuration, the acceleration input remains for 10 seconds and drops to zero.

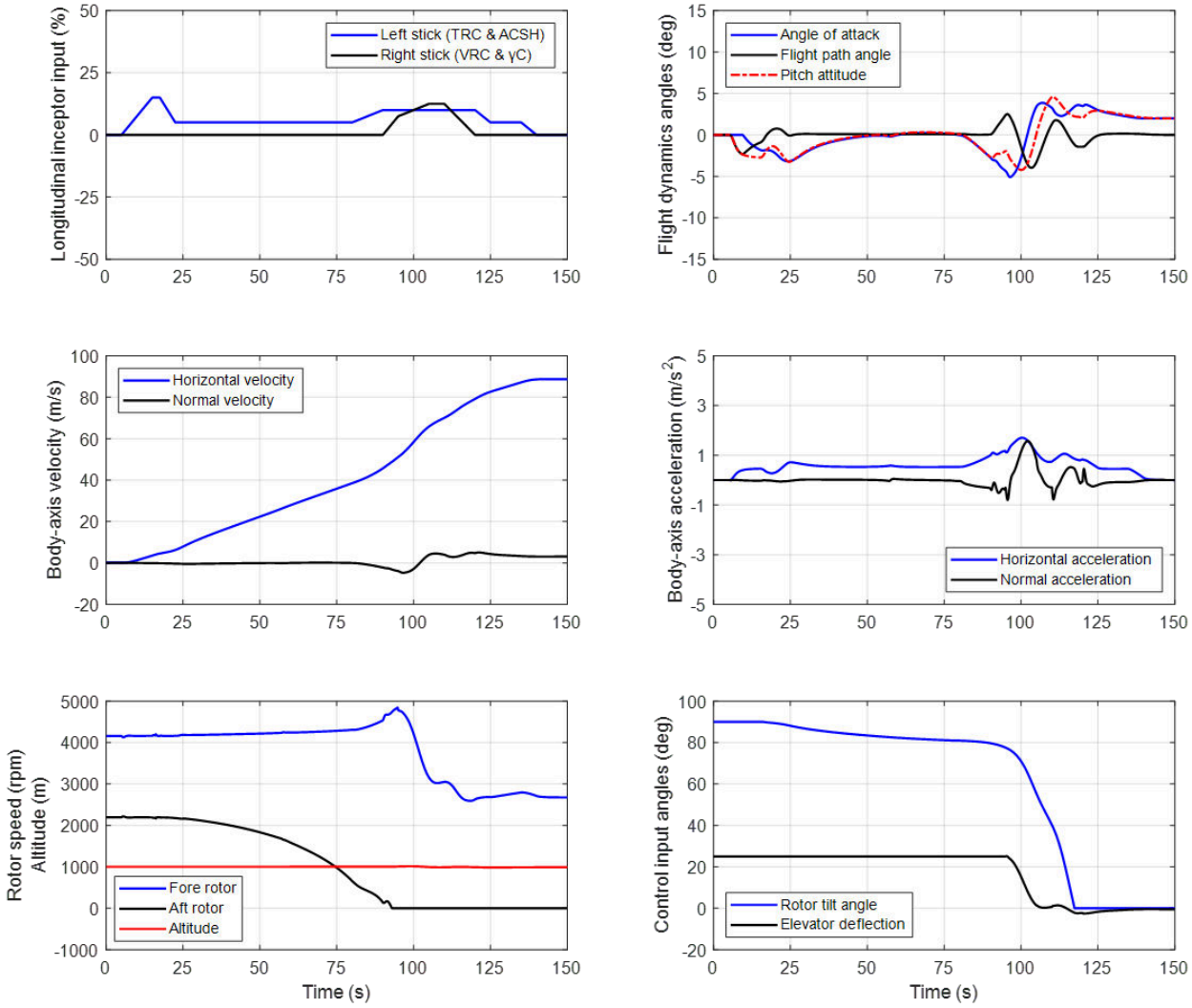

Fig. 22 Flight dynamics response during the full conversion - longitudinal inceptor inputs, body-axis velocity, rotor rpm, altitude, control inputs, body-axis acceleration, and flight dynamics angles

No extreme change in altitude and pitch attitude confirms that the SCAS design leads to a successful conversion flight. TRC and blending regime produce a negative pitch attitude at the early stage due to control strategy. Afterwards, an acceleration of 0.05 g is followed as commanded and the flight does not include a negative pitch attitude. However, when the left stick input increases to 10 percent, pitch attitude falls to -5 deg. This shows that the smaller amount of acceleration during the conversion can be made with a positive pitch attitude at a given rotor tilt angle, even though the control strategy is to pitch down and increase airspeed. At the stall speed, the aft rotor is ideally disengaged because aft thrust at a positive pitch attitude will result in a large drag force. Compared to arbitrary elevator input, the maximum elevator deflection that generates greater aerodynamic lift only leads to no-use aft thrust at the stall speed, which the neutral position of the elevator could not achieve. After control allocation to the wing borne mode is finished above the stall speed, a tilt rate is rapid (between 90 and 115 seconds). The rapid tilt rate introduces unsteady flight dynamics so

that large deviations of both altitude and pitch attitude up to 10 m and 5 deg occur during the rapid tilt change period. Since the flight path angle response always lags behind pitch attitude, controlling flight path angle means that it is difficult to attenuate disturbances. A tilt rate limit of 7.5 deg s^{-1} was imposed on the tilt schedule and a higher tilt rate limit resulted in a greater amount of inceptor input to compensate for the disturbance between 50 and 75 m s^{-1}.

VI. Conclusion

The paper presents the optimum tilt schedule to encompass the helicopter, conversion, and fixed-wing aircraft configurations with no flight state switch in the cockpit, but automatically scheduled on airspeed. Trim analysis for the steady wings level flight reveals that the relative stability can map out the conversion corridor. The proposed conversion corridor should also consider the dynamic optimisation and manoeuvres such as climb, descent and turn, which the paper has not covered. The four flight cases and their handling quality ratings hinged on the shape of the tilt schedule. In the subsequent assessment of the bandwidth and quickness criterion, it was observed that the speed of response had a proportional relationship with the bandwidth frequency.

A tilt-scheduled conversion flight simulation still requires pilot compensation to maintain the altitude change due to nonlinearity without excessive pitch attitude. If the tilt rate limit is too high, higher altitude compensation from the right stick is required. To deal with intrusive unsteady dynamics under a high tilt rate, pitch attitude response may be suitable for a tilt-scheduled flight control system rather than flight path angle response type. This is because a faster response is expected to reduce pilot workload and enhance passenger comfort with a constant pitch attitude during conversion. In the helicopter mode, the acceleration control strategy is to pitch down the aircraft. However, low acceleration may have a positive pitch attitude depending on the current rotor tilt angle along a tilt schedule.

Above the stall speed, the aft rotor thrust is redundant because the maximum elevator deflection is made at the beginning. However, the minimum elevator deflection that results in no-use aft rotor thrust at the stall speed should be specified to provide the elevator with a control margin. If the initial elevator deflection leads to zero aft thrust faster than or closer to the stall speed, it is expected that the smaller airspeed for the primary control switch benefits the power savings of the aircraft by replacing powered lift with aerodynamic forces. Furthermore, the first zero-thrust airspeed should try to match the airspeed for the primary control switch. Otherwise, controllability between the two points will be challenged because aft rotor thrust will not function at a demanded stick input. Lastly, the point on the tilt schedule at which the tilt rate becomes large should be almost the airspeed for the primary control switch because a high tilt angle is not suitable for the fixed-wing aircraft control scheme.

In future work, a second-order tilting actuator system model should be considered for a more accurate design of the tilt schedule and the optimum tilt rate needs to be determined to avoid stressing the conversion actuator with a high duty cycle. Given that the ride quality relies not only on acceleration but also frequency [42], the optimum choice for weighted sum and aerodynamic derivatives analysis could be taken into account for conversion corridor to minimise expected pilot workload on flight path gamma control. Lastly, a piloted simulation will be conducted to compare the handling qualities of the tilt-scheduled flight control system with the predicted handling quality ratings.

References

[1] Lu, K., Tian, H., Zhen, P., Lu, S., and Chen, R., "Conversion Flight Control for Tiltrotor Aircraft via Active Disturbance Rejection Control," *Aerospace*, Vol. 9, No. 3, 2022. https://doi.org/10.3390/aerospace9030155.

[2] Naldi, R., and Marconi, L., "Optimal Transition Maneuvers for a Class of V/STOL Aircraft," *Automatica*, Vol. 47, No. 5, 2011, pp. 870–879. https://doi.org/https://doi.org/10.1016/j.automatica.2011.01.027.

[3] Maisel, M., Giulianetti, D., and Dugan, D., *The History of the XV-15 Tilt Rotor Research Aircraft: From Concept to Flight*, No. 17 in Monographs in Aerospace History, National Aeronautics and Space Administration, Office of Policy and Plans, NASA History Division, Washington, DC, 2000.

[4] Fortenbaugh, R., and Lazaric, L., "BA609 Handling Qualities; Development Flight Test Results," *RAeS Rotorcraft Handling Qualities Conference*, Royal Aeronautical Society, Liverpool, England, 2008.

[5] Dunford, P., Lunn, K., Magnuson, R., and Marr, R., "The V-22 Osprey - A Significant Flight Test Challenge," *16th European Rotorcraft Forum*, Royal Aeronautical Society, Glasgow, United Kingdom, 1990.

[6] Liu, Z., He, Y., Yang, L., and Han, J., "Control Techniques of Tilt Rotor Unmanned Aerial Vehicle Systems: A Review," *Chinese Journal of Aeronautics*, Vol. 30, No. 1, 2017, pp. 135–148. https://doi.org/https://doi.org/10.1016/j.cja.2016.11.001.

[7] Franklin, J., *Dynamics, Control, and Flying Qualities of V/STOL Aircraft*, AIAA Education Series, American Institute of Aeronautics and Astronautics, Reston, VA, 2002.

[8] Padfield, G. D., *Helicopter Flight Dynamics: Including a Treatment of Tiltrotor Aircraft*, 3rd ed., Aerospace Series, John Wiley & Sons, Hoboken, NJ, 2018.

[9] Ducard, G. J., and Allenspach, M., "Review of Designs and Flight Control Techniques of Hybrid and Convertible VTOL UAVs," *Aerospace Science and Technology*, Vol. 118, 2021, p. 107035. https://doi.org/https://doi.org/10.1016/j.ast.2021.107035.

[10] Bauersfeld, L., and Ducard, G., "Fused-PID Control for Tilt-rotor VTOL Aircraft," *2020 28th Mediterranean Conference on Control and Automation (MED)*, IEEE, St Raphaël, France, 2020, pp. 703–708.

[11] Sato, M., and Muraoka, K., "Flight Controller Design and Demonstration of Quad-Tilt-Wing Unmanned Aerial Vehicle," *Journal of Guidance, Control, and Dynamics*, Vol. 38, No. 6, 2015, pp. 1071–1082. https://doi.org/10.2514/1.G000263.

[12] Okan, A., Tekinalp, O., and Kavsaoglu, M., "Flight Control of a Tilt-Duct UAV," *1st UAV Conference 2002*, Portsmouth, VA, 2002, p. 3466.

[13] Kang, Y., Park, B., Yoo, C., Kim, Y., and Koo, S., "Flight Test Results of Automatic Tilt Control for Small Scaled Tilt Rotor Aircraft," *2008 International Conference on Control, Automation and Systems*, IEEE, Seoul, 2008, pp. 47–51.

[14] Liu, Z., Theilliol, D., Yang, L., He, Y., and Han, J., "Transition Control of Tilt Rotor Unmanned Aerial Vehicle Based on Multi-Model Adaptive Method," *2017 International Conference on Unmanned Aircraft Systems (ICUAS)*, IEEE, Miami, FL, 2017, pp. 560–566.

[15] Grzędziński, K., Stéphan, V., and Zolotas, A. C., "Wing Tilt Scheduling in Tandem-wing VTOL Configurations," *9th Biennial Autonomous VTOL Technical Meeting*, Virtual Event, 2021.

[16] Song, Y., and Wang, H., "Design of Flight Control System for a Small Unmanned Tilt Rotor Aircraft," *Chinese Journal of Aeronautics*, Vol. 22, No. 3, 2009, pp. 250–256. https://doi.org/https://doi.org/10.1016/S1000-9361(08)60095-3.

[17] Vigano, L., Riccardi, F., and Leonello, D., "Development of Augmented Control Laws for a Tiltrotor in Low and High Speed Flight Modes," *43rd European Rotorcraft Forum*, Vol. 1, Milan, Italy, 2017, pp. 438–451.

[18] Nonami, K., Kendoul, F., Suzuki, S., Wang, W., and Nakazawa, D., *Autonomous Flying Robots: Unmanned Aerial Vehicles and Micro Aerial Vehicles*, Springer, Tokyo, 2010, Chaps. Development of Autonomous Quad-Tilt-Wing (QTW) Unmanned Aerial Vehicle: Design, Modeling, and Control, pp. 77–93.

[19] Çetinsoy, E., Dikyar, S., Hançer, C., Oner, K., Sirimoglu, E., Unel, M., and Aksit, M., "Design and Construction of a Novel Quad Tilt-Wing UAV," *Mechatronics*, Vol. 22, No. 6, 2012, pp. 723–745. https://doi.org/https://doi.org/10.1016/j.mechatronics.2012.03.003.

[20] Öner, K. T., Çetinsoy, E., Sirimoğlu, E., Hancer, C., Ünel, M., Akşit, M. F., Gülez, K., and Kandemir, I., "Mathematical Modeling and Vertical Flight Control of a Tilt-Wing UAV," *Turkish Journal of Electrical Engineering & Computer Sciences*, Vol. 20, No. 1, 2012, pp. 149–157. https://doi.org/10.3906/elk-1007-624.

[21] Papachristos, C., Alexis, K., and Tzes, A., "Design and Experimental Attitude Control of an Unmanned Tilt-Rotor Aerial Vehicle," *15th International Conference on Advanced Robotics (ICAR)*, Tallinn, Estonia, 2011, pp. 465–470.

[22] Papachristos, C., Alexis, K., and Tzes, A., "Towards a High-End Unmanned Tri-Tiltrotor: Design, Modeling and Hover Control," *20th Mediterranean Conference on Control & Automation (MED)*, IEEE, Barcelona, Spain, 2012, pp. 1579–1584.

[23] Perfect, P., Jump, M., and White, M. D., "Handling Qualities Requirements for Future Personal Aerial Vehicles," *Journal of Guidance, Control, and Dynamics*, Vol. 38, No. 12, 2015, pp. 2386–2398. https://doi.org/10.2514/1.G001073.

[24] Hart, S. G., and Staveland, L. E., "Development of NASA-TLX (Task Load Index): Results of Empirical and Theoretical Research," *Human Mental Workload*, Advances in Psychology, Vol. 52, North-Holland, 1988, pp. 139–183.

[25] Perfect, P., Jump, M., and White, M. D., "Methods to Assess the Handling Qualities Requirements for Personal Aerial Vehicles," *Journal of Guidance, Control, and Dynamics*, Vol. 38, No. 11, 2015, pp. 2161–2172. https://doi.org/10.2514/1.G000862.

[26] Dollinger, D., Reiss, P., Angelov, J., Löbl, D., and Holzapfel, F., "Control Inceptor Design for Onboard Piloted Transition VTOL Aircraft Considering Simplified Vehicle Operation," *AIAA Scitech 2021 Forum*, Virtual Event, 2021, p. 1896.

[27] Meyer, M. A., and Padfield, G. D., "First Steps in the Development of Handling Qualities Criteria for a Civil Tilt Rotor," *Journal of the American Helicopter Society*, Vol. 50, No. 1, 2005, pp. 33–45. https://doi.org/10.4050/1.3092841.

[28] U.S. Department of Defense, "Military Standard - Flying Qualities of Piloted Airplanes," Tech. Rep. MIL-STD-1797A, U.S. Department of Defense, 1990.

[29] Aviation Engineering Directorate, "Aeronautical Design Standard Performance Specification Handling Qualities Requirements for Military Rotorcraft," Tech. Rep. ADS-33E-PRF, U.S. Army Aviation and Missile Command, 2000.

[30] Dollinger, D., Fricke, T., and Holzapfel, F., "Control Inceptor Design for Remote Control of a Transition UAV," *AIAA Aviation 2019 Forum*, 2019, p. 3268.

[31] Valdés, G., "Urban Air Mobility Flight Dynamics," M.Sc. Dissertation, School of Aerospace, Transport and Manufacturing, Cranfield University, Cranfield, Bedfordshire, 2020.

[32] Mark, D., and Harold, Y., AVL, Ver 3.36. Massachusetts Institute of Technology, Cambridge, MA, 2017. URL https://web.mit.edu/drela/Public/web/avl/.

[33] Mark, D., QPROP, Ver 1.22. Massachusetts Institute of Technology, Cambridge, MA, 2007. URL https://web.mit.edu/drela/Public/web/qprop/.

[34] Chappell, D., "In-Plane Forces and Moments on Installed Inclined Propellers at Low Forward Speeds," Tech. Rep. ESDU 89047 Amendment E, Engineering Sciences Data Unit, 2021.

[35] Rinalducci, E. J., "Effects of Aircraft Motion on Passengers' Comfort Ratings and Response Times," *Perceptual and Motor Skills*, Vol. 50, No. 1, 1980, pp. 91–97. https://doi.org/10.2466/pms.1980.50.1.91.

[36] Cook, M., *Flight Dynamics Principles: A Linear Systems Approach to Aircraft Stability and Control*, 3rd ed., Aerospace Engineering, Butterworth-Heinemann, Waltham, MA, 2013.

[37] EASA, "Means of Compliance with the Special Condition VTOL," Tech. Rep. MOC SC-VTOL, European Aviation Safety Agency, May 2021.

[38] EASA, "Second Publication of Means of Compliance with the Special Condition VTOL," Tech. Rep. MOC-2 SC-VTOL, European Aviation Safety Agency, Jun. 2022.

[39] EASA, "Third Publication of Proposed Means of Compliance with the Special Condition VTOL," Tech. Rep. MOC-3 SC-VTOL, European Aviation Safety Agency, Jun. 2022.

[40] EASA, "Final Special Condition SC E-19 - Electric / Hybrid Propulsion System," Tech. Rep. SC E-19, European Aviation Safety Agency, Apr. 2021.

[41] FAA, "Federal Aviation Regulations Part 21 — Certification Procedures for Products and Articles," Tech. rep., Federal Aviation Administration, Jan. 2021.

[42] Edwards, T., and Price, G., "eVTOL Passenger Acceptance," Tech. Rep. ARC-E-DAA-TN76992, NASA Ames Research Center, 2020.